

# Investigation of arsenic-doped ZnO thin films grown on Si substrate by atmospheric-pressure metal-organic chemical vapor deposition

S. C. Hung<sup>\*1</sup>, K. J. Wang<sup>2</sup>, S. M. Lan<sup>2,3</sup>, T. N. Yang<sup>3</sup>, W. Y. Uen<sup>2</sup>, and G. C. Chi<sup>4</sup>

<sup>1</sup>Optical Science Center, National Central University, Zhong-Li 320, Taiwan

<sup>2</sup>Department of Electronic Engineering, College of Electrical Engineering and Computer Science, Chung-Yuan Christian University, Chung-Li 32023, Taiwan

<sup>3</sup>Institute of Nuclear Energy Research Atomic Energy Council, Longtan, Taoyuan 32546, Taiwan

<sup>4</sup>Department of Photonics, National Chiao Tung University, Hsinchu 300, Taiwan

Received 31 May 2011, revised 3 November 2011, accepted 23 January 2012

Published online 22 February 2012

**Keywords** annealing, doping, MOCVD, zinc oxide

\* Corresponding author: e-mail shengchun@ufl.edu, Phone: (+886)3-4227151 ext. 57900, Fax: (+886)3-4258816

Zinc oxide (ZnO) thin film was grown on semi-insulating Si substrate using arsine (AsH<sub>3</sub>) as precursor by atmospheric-pressure metal-organic chemical vapor deposition (AP-MOCVD). In recently reported results, the physical mechanisms for As-doped ZnO thin films are explained as As substitution for oxygen (As<sub>O</sub>) or As substitution for Zn and As combined with two Zn vacancies (As<sub>Zn</sub>-2V<sub>Zn</sub>). In this study, we control the *in situ* annealing ambient into two environments with various

temperatures, which are Zn-rich, using diethylzinc (DEZn) as ambient gas, and O-rich, using water vapor as ambient gas, respectively. This should help to create As<sub>O</sub> and As<sub>Zn</sub>-2V<sub>Zn</sub>. The ZnO thin film after *in situ* thermal annealing with H<sub>2</sub>O vapor ambient at 550 and 750 °C show p-type conductivity with hole concentration of  $2.651 \times 10^{17}$  and  $1.782 \times 10^{18} \text{ cm}^{-3}$ , Hall mobilities of 10.08 and 5.402 cm<sup>2</sup>/V s, and resistivities of 2.368 and 0.6485 Ω cm, respectively.

© 2012 WILEY-VCH Verlag GmbH & Co. KGaA, Weinheim

**1 Introduction** Zinc oxide (ZnO) has attracted a lot of attention because of its large direct bandgap of 3.37 eV and high exciton binding energy of 60 meV at room temperature (RT), which make it a promising candidate for the applications in highly efficient and stable RT ultraviolet (UV) lasers and light-emitting diodes (LEDs) [1–6]. However, there is a difficulty in achieving reliable and reproducible p-type conductivity for ZnO material. It has been proven that it is very difficult to dope shallow acceptor levels in ZnO because of the compensation effect of native n-type carriers released by the donor-type defects such as oxygen vacancies and zinc interstitials. Based on the basic concept that the holes can be created by substituting oxygen anions with group-V elements. Many groups have tried to dope ZnO using group-V elements, such as N, P, As, and Sb [7–13]. Theoretically speaking, N is the most promising candidate because of its comparable atomic radius to O and the lowest hole ionization energy compared to other group-V elements. Unfortunately, the ionization energy of N was

observed to be rather large, around 170–200 meV, which resulted in a low hole concentration.

Arsenic is another promising element for ZnO p-type doping because of its substitution mechanisms. Two different explanations were reported that As might replace the O site and form As<sub>O</sub> [14], this substituted As atom has a valence state of (–3) in the divalent O site. Therefore, one hole is generated in order to accomplish charge neutrality. The other theoretical model proposed is that As occupies Zn sites and forms As<sub>Zn</sub>-2V<sub>Zn</sub> [15], which produces an acceptor level, presumably shallower than that of As<sub>O</sub> [16].

In this study, we demonstrate the use of two different *in situ* annealing ambients with various temperatures in order to help create As<sub>O</sub> and As<sub>Zn</sub>-2V<sub>Zn</sub> in the As-doped ZnO thin film, and show that p-type ZnO is available with As<sub>Zn</sub>-2V<sub>Zn</sub> in it under certain annealing temperatures.

**2 Experimental** The As-doped ZnO thin films were grown on Si (111) substrates by an atmospheric-pressure

chemical vapor deposition system. Diethylzinc (DEZn), arsine ( $\text{AsH}_3$ ), and water vapor were used as the precursors of Zn, As, and O, respectively.  $\text{N}_2$  was used as the carrier gas. Because the lattice mismatches between ZnO and Si (111) and Si (100) are about 15 and 40%, respectively [17, 18], before growing As-doped ZnO thin films, an undoped ZnO buffer layer that is around 10–20 nm was grown at low temperature (LT) of 180 °C with a gas-flow ratio of  $[\text{H}_2\text{O}]:[\text{DEZ}] = 13$  for 8 min. For growth of the As-doped ZnO layer, the growth temperature and [VI]/[II] ratio were kept at 450 °C and 2.7, respectively. The time for ZnO thin-film growth was set for 30 min with the doping gas flow ( $\text{AsH}_3$ ) rate at 372  $\mu\text{mol}/\text{min}$ . In order to investigate the effect of annealing temperature in different ambients, As-doped ZnO were *in situ* postannealed in  $\text{H}_2\text{O}$  vapor or DEZn ambient at various temperatures for 25 min from 550 to 750 °C. Photoluminescence (PL) spectra were measured with a continuous-wave He–Cd 325 nm laser with a power density incident on the samples of  $\sim 1 \text{ W}/\text{cm}^2$ . Emission from the sample was dispersed by an Acton Research Corp. SP275 monochromator and detected by a Hamamatsu R928 photomultiplier tube triggered with a Stanford Research Systems SR830 lock-in amplifier. X-ray diffraction (XRD) measurement was carried out on X'Pert diffractometer system, using with  $\text{Cu K}\alpha_1$  radiation. Scanning electron microscopy (SEM) was employed to examine the morphology of the samples.

**3 Results and discussion** Figures 1 and 2 show the SEM surface and cross-sectional images of As-doped ZnO thin films deposited on Si (111) substrates at different postannealing temperatures in the DEZn and  $\text{H}_2\text{O}$  vapor ambient, respectively. As shown in Fig. 1 and, there are a lot of irregular sheet islands on the as-grown ZnO thin film.

When the postannealing temperature was raised, the thickness of As-doped ZnO film decreased abruptly to one half and the surface became smoother in both cases, which indicated that the As-doped ZnO thin film were regrown along the horizontal direction during the postanneal process.

Images of As-doped ZnO films with postannealing temperatures from 550 to 700 °C in DEZn ambient are shown in Fig. 1. Lots of irregular strip-shaped island structures are shown on the surface without any postthermal treatment. When the as-grown As-doped ZnO thin films were postthermally treated at different temperatures although the thickness became less, which indicated that the As-doped ZnO thin films were regrown along the horizontal direction, the structure of the thin film shows a lot of voids inside, as shown in the SEM images. This might increase the surface and generate lots of defects and dangling bonds that caused n-type behavior in these samples.

For the As-doped ZnO thin films with postthermal treatment using various temperatures in water vapor ambient, as the annealing temperature increased, regrowth of As-doped ZnO along the horizontal direction can be observed via the SEM top and cross-sectional images. As shown in Fig. 2, a smooth surface with large grain boundary can be achieved using 550 and 750 °C. On the other hand, the sample postannealed using 600, 650, and 700 °C shows a much reduced thickness (around 1/3 of the original thickness) and small grains. Overall, postheat treatment can help as-grown As-doped ZnO to regrow along the horizontal direction. Using water vapor ambient will help each grain to become attached to each other and produce a smooth surface compared with the one using DEZn ambient.

The optical properties of As-doped ZnO thin films were investigated by PL measurements at room temperature (RT) and LT, as shown in Fig. 3. Figure 3a shows the RT-PL

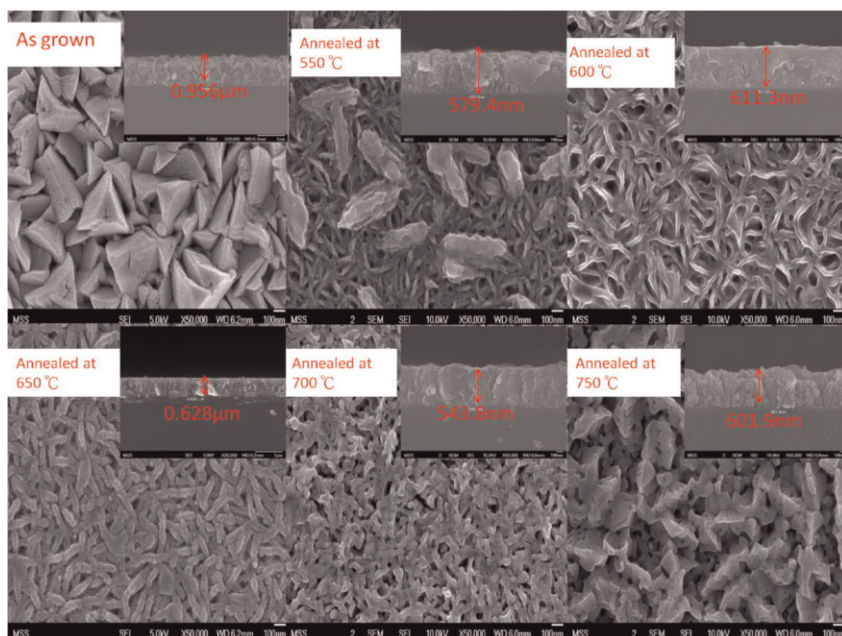


**Figure 1** (online color at: [www.pss-a.com](http://www.pss-a.com)) SEM images of ZnO thin film with postannealed treatment at various temperatures in DEZn ambient.

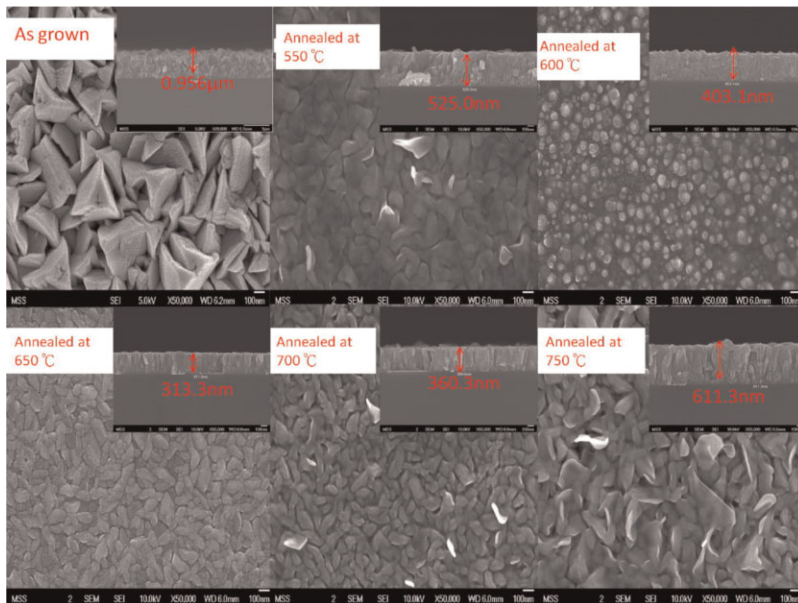


**Figure 2** (online color at: [www.pss-a.com](http://www.pss-a.com)) SEM images of ZnO thin film with postannealed treatment at various temperatures in H<sub>2</sub>O vapor ambient.

spectra of As-doped ZnO thin films grown on Si (111) substrates with different postannealing temperatures in DEZn ambient. Two distinct peaks are seen corresponding to the near band edge (NBE) emission caused by exciton-related emission around 3.2 eV [19, 20] and the deep level (DL) emission band that was attributed by oxygen vacancies (V<sub>O</sub>) or zinc interstitials (Zn<sub>i</sub>) around 2.5 eV [21, 22]. However, as the annealing temperature increased, the intensity of the NBE emission increases, which indicates that the crystal quality of the film was improved with increasing annealing temperature. In addition, as the annealing temperatures increased, the peak shows a redshift

from 3.292 to 3.278 and 3.263 eV, which might be caused by lattice distortion because of the As atoms in the ZnO lattice structure. On the other hand, when the annealing temperature increased, the DL emission will not vanish because the material structure still roughened and the defect density was still high, as shown in the SEM images.

Figure 3b shows the RT-PL results of the ZnO thin films with postannealed in water vapor ambient. The NBE emission around 3.2 eV caused by the exciton-related emission was observed. The as-grown ZnO thin film exhibited a very weak NBE emission at 3.292 eV, as the annealing temperature increased, the intensity of the NBE

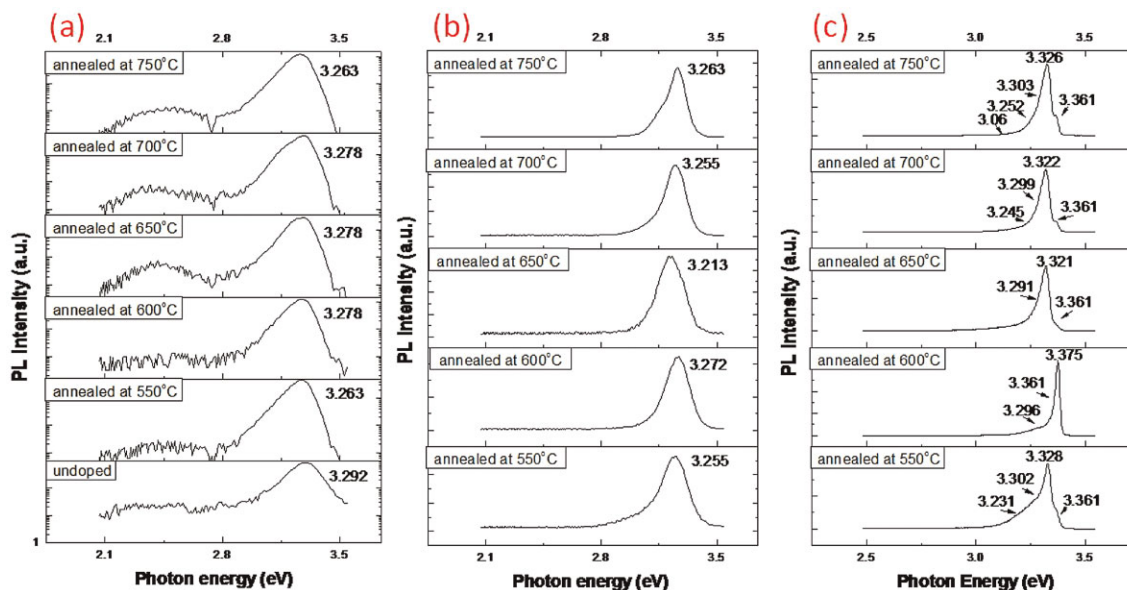


**Figure 3** PL results of ZnO thin film with postannealed treatment at various temperatures in different ambients. (a) In DEZn ambient at room temperature, (b) in H<sub>2</sub>O vapor ambient at room temperature, (c) in H<sub>2</sub>O vapor ambient at low temperature (14 K).



emission around 3.292 eV becomes bigger. This indicates that the crystal quality of the thin film was improved with increasing annealing temperature. In addition, as the annealing temperatures increased, the PL peak wavelength also shows a redshift from 3.292 to 3.272–3.213 eV. The narrowing of the bandgap after annealing can be ascribed to the following effects of a merging of the impurity band with the valence or conduction band due to the heavy doping of As. In order to investigate the influence of annealing treatment on the optical properties of the films in more detail, a LT (14 K) PL measurement was performed on the As-doped ZnO films. Figure 3c shows that the LT-PL spectra of p-type ZnO film annealed at 550 °C exhibits four emission peaks at 3.361, 3.328, 3.302, and 3.231 eV, respectively. The emission peak at 3.361 eV can be assigned to a neutral donor-bound exciton ( $D^0X$ ) [23]. The peak at 3.328 eV has been previously identified as a neutral acceptor-bound exciton ( $A^0X$ ) [24–26]. The peak at 3.302 eV is attributed to the recombination emissions between free electrons and acceptor holes (FA) [24–26]. This suggested that some arsenic-related acceptors existed in the ZnO film. The peak at 3.231 eV is due to the recombination of donor–acceptor pairs (DAP) [24–27]. This also suggests that acceptors were formed in As-doped ZnO thin film. Meanwhile, the results of Hall measurement also demonstrate that the film has p-type conductivity. The As-doped ZnO thin films that were postannealed at 600 °C showed the emission wavelength at 3.375 eV could be caused by the first excited state transitions ( $n = 1$ ) of free excitons (FX) [28]. The peaks at 3.361 and 3.296 eV are assigned to the  $D^0X$  and FA. So the film exhibited strong n-type conductivity. On the other hand, the films postannealed at temperatures from 650 to 750 °C show some emission peaks at 3.361 eV, assigned to  $D^0X$ , 3.321–3.326 eV, assigned to  $A^0X$ , 3.291–3.303 eV, assigned to the FA transition, and 3.245 and 3.252 eV are considered to be

due to the DAP transition, respectively. The LT-PL results showed that the FA and DAP emissions became larger for the film annealed at 750 °C, while its electrical properties show p-type character. We believe that this could be caused by the influence of zinc vacancies ( $V_{Zn}$ ) [29].

The acceptor energy of the arsenic dopant can be estimated from the following equation [30]:  $E_A = E_g - E_{FA} + k_B T/2$ , where  $E_g$  and  $E_{FA}$  are the intrinsic bandgap and free electron-acceptor level transition, respectively. In the study,  $E_{FA}$  has been measured to be around 3.302 eV at 14 K. With  $E_g = 3.437$  eV, the value of  $E_A$  should be 135 meV, which is close to the reported value of 150 meV using the  $As_{Zn} - 2V_{Zn}$  model [16]. Researchers have found that arsenic substitution O ( $As_O$ ) has a high formation energy and acceptor-ionization energies of about 930 meV above the valence-band maximum, thereby it is difficult to provide sufficient holes in the doping model of  $As_O$  [16].

Figure 4a and b shows the XRD results with thin films postannealed in the DEZn and water vapor ambient, respectively. As shown in Fig. 4a, all films exhibit polycrystalline structure and not preferred  $c$ -axis orientation, which means the energy for lateral growth was not enough to improve the crystal quality of As-doped ZnO. These results correspond to the SEM images and PL data mentioned above. In addition, it should be noted that the preferential orientation of the films is (101) but not (002), which was indicated by most other papers. This could be because of the LT-grown buffer layer (180 °C) causes it to grow along (101) more easily. For the sample annealed in water ambient, we still saw polycrystalline structured ZnO films, as shown in Fig. 4b. XRD patterns show that the films were grown along a preferred orientation (101), which could be caused by the Si (111) substrate. An interesting phenomenon was observed when the postheat-treatment temperature was raised under water vapor ambient, the intensity of the peak (002)

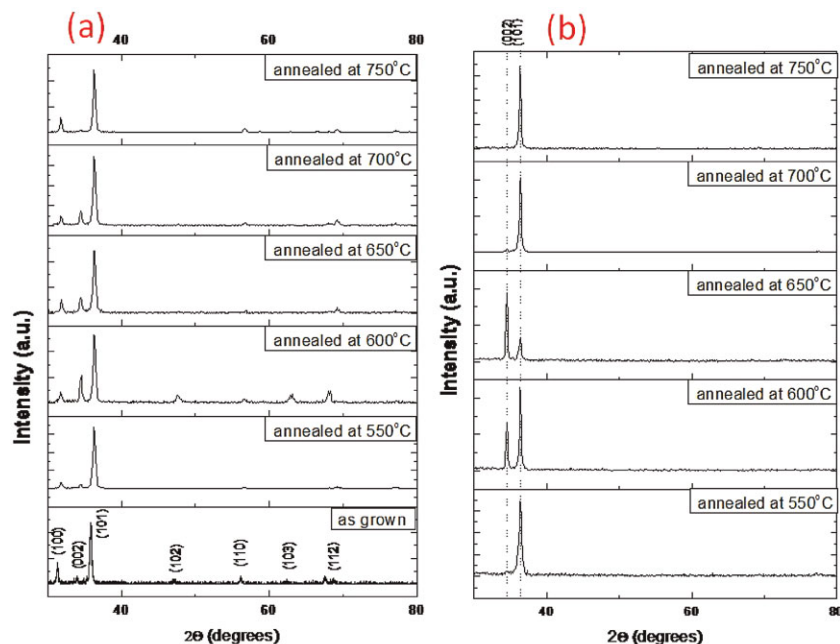


**Figure 4** XRD results of ZnO thin film with postannealing treatment at various temperatures in different ambient. (a) In DEZn ambient at room temperature (b) in  $H_2O$  vapor ambient at room temperature.

**Table 1** Hall measurement results of As-doped ZnO films with different annealing temperatures in DEZn ambient.

| annealing temperature (°C) | resistivity ( $\Omega$ cm) | mobility ( $\text{cm}^2/\text{V s}$ ) | carrier concentration ( $\text{cm}^{-3}$ ) | type |
|----------------------------|----------------------------|---------------------------------------|--|------|
| 550                        | 0.7267                     | 3.75                                  | $-2.291 \times 10^{18}$                    | n    |
| 600                        | 0.1798                     | 9.088                                 | $-3.821 \times 10^{18}$                    | n    |
| 650                        | 0.06461                    | 19.58                                 | $-4.933 \times 10^{18}$                    | n    |
| 700                        | 0.1361                     | 10.21                                 | $-4.644 \times 10^{18}$                    | n    |
| 750                        | 0.2964                     | 11.61                                 | $-1.814 \times 10^{18}$                    | n    |

increased, which was evidenced from the SEM cross-sectional image that the thickness reduced when the postannealing temperature was raised. For the samples with postannealing temperatures of 550 and 750 °C, only the (101) direction can be observed, which showed that it is very difficult to dope As into ZnO thin film if the direction of ZnO growth is along (002). This could explain the difference between the defect density along these two directions.

Table 1 shows the resistivity, carrier concentration, and Hall mobility of As-doped ZnO films as a function of the annealing temperature in DEZn atmosphere. The undoped ZnO thin film shows n-type conductivity, with resistivity, Hall mobility, and electron concentration as 0.2464  $\Omega$  cm, 13.47  $\text{cm}^2/\text{V s}$ , and  $1.881 \times 10^{18} \text{ cm}^{-3}$ , respectively. As is known, the n-type conductivity of ZnO is ascribed to the influence of native donor defects such as oxygen vacancies ( $\text{V}_\text{O}$ ) or zinc interstitials ( $\text{Zn}_\text{i}$ ). On the other hand, arsenic is a p-type dopant that replaces a zinc vacancy or an oxygen site to form complexes of the type  $\text{As}_{\text{Zn}}-2\text{V}_{\text{Zn}}$  and  $\text{Zn}_3\text{As}_2$  in ZnO, respectively. In this study, we adopt the Zn-rich DEZn at a flow rate of 2.0031  $\mu\text{mol}/\text{min}$  under annealing conditions with the  $\text{AsH}_3$  flow rate 124  $\mu\text{mol}/\text{min}$  in this experiment and expect to obtain complexes of the type  $\text{Zn}_3\text{As}_2$  by  $\text{As}_\text{O}$ . This mechanism can contribute to the hole concentration. However, in Table 1, it can be seen that the carrier concentration of As-doped ZnO thin films still showed n-type conductivity with high electron concentrations of  $10^{18} \text{ cm}^{-3}$ . Obviously, the As atoms in the films have a tendency to occupy interstitial sites as neutral defects, and arsenic substitution for oxygen ( $\text{As}_\text{O}$ ) is very difficult to achieve.

Table 2 shows the resistivity, carrier concentration, and Hall mobility of As-doped ZnO films as a function of annealing temperature in  $\text{H}_2\text{O}$  vapor atmosphere. The undoped ZnO thin film shows n-type resistivity, Hall mobility, and electron concentration as 0.2464  $\Omega$  cm, 13.47  $\text{cm}^2/\text{V s}$ , and  $1.881 \times 10^{18} \text{ cm}^{-3}$ , respectively. In this study, we adopt the O-rich  $\text{H}_2\text{O}$  vapor at a flow rate of 18.28  $\mu\text{mol}/\text{min}$  under annealing conditions with an  $\text{AsH}_3$  flow of rate of 31  $\mu\text{mol}/\text{min}$ , which is expected to support the formation of  $\text{As}_{\text{Zn}}$  to form complexes of the type  $\text{As}_{\text{Zn}}-2\text{V}_{\text{Zn}}$ . This mechanism can contribute to the hole concentration. In Table 2, it can be seen that the carrier concentration of As-doped ZnO films at annealing temperatures of 550 and

**Table 2** Hall measurement results of As-doped ZnO films with different annealing temperatures in  $\text{H}_2\text{O}$  vapor ambient.

| annealing temperature (°C) | resistivity ( $\Omega$ cm) | mobility ( $\text{cm}^2/\text{V s}$ ) | carrier concentration ( $\text{cm}^{-3}$ ) | type |
|----------------------------|----------------------------|---------------------------------------|--|------|
| 550                        | 2.368                      | 10.08                                 | $2.651 \times 10^{17}$                     | p    |
| 600                        | 0.01315                    | 14.93                                 | $-3.197 \times 10^{19}$                    | n    |
| 650                        | 0.1065                     | 7.325                                 | $-8 \times 10^{18}$                        | n    |
| 700                        | 0.6219                     | 1.832                                 | $-5.479 \times 10^{18}$                    | n    |
| 750                        | 0.6485                     | 5.402                                 | $1.782 \times 10^{18}$                     | p    |

750 °C, show p-type conductivity with hole concentrations of  $2.651 \times 10^{17}$  and  $1.782 \times 10^{18}$ , respectively. It is very interesting to note that the conductivity of ZnO films converts to p-type. However, the films returned to strong n-type conductivity at annealed temperatures from 600 to 700 °C. The increase of electron concentration may be due to the formation of donors ( $\text{As}_{\text{Zn}}$  and  $\text{As}_{\text{Zn}}-\text{V}_{\text{Zn}}$ ) and a large number of donor point defects (oxygen vacancies and zinc interstitials). Moreover, the hole concentration is insufficient to compensate the high background electron concentration, hence the ZnO film is still n-type.

**4 Conclusion** In conclusion, As-doped ZnO thin films with postannealing in DEZ and water vapor ambient were studied. The p-ZnO were observed under conditions of annealing in  $\text{H}_2\text{O}$  vapor ambient at 550 and 750 °C. We believe that the growth direction will cause different levels of defect density, which might generate some influence on the electrical properties of ZnO. The doping mechanism of As in ZnO could be easily achieved for the  $\text{As}_{\text{Zn}}-2\text{V}_{\text{Zn}}$  complex doping mechanism in ZnO with a water vapor postannealed ambient.

## References

- [1] U. Rau and M. Schmidt, *Thin Solid Films* **387**, 141 (2001).
- [2] K. Keis, E. Magnusson, H. Lindstrom, S. E. Lindquist, and A. Hagfeldt, *Sol. Energy Mater. Sol. Cells* **73**, 51 (2002).
- [3] Y. Liu, C. R. Gorla, S. Liang, N. Emanetoglu, Y. Lu, H. Shen, and M. Wraback, *J. Electron. Mater.* **29**, 60 (2000).
- [4] C. Weisbuch, H. Benisty, and R. J. Houdre, *J. Lumin.* **85**, 271 (2000).
- [5] S. C. Jain, M. Willander, J. Narayan, and R. Van Overstraeten, *J. Appl. Phys.* **87**, 965 (2000).
- [6] S. J. Pearton, D. P. Norton, K. Ip, Y. W. Heo, and T. Steiner, *Prog. Mater. Sci.* **50**, 293 (2005).
- [7] S. Kohiki, M. Nishitani, and T. Wada, *J. Appl. Phys.* **75**, 2069 (1994).
- [8] W. W. Wenas, A. Yamada, and K. Takehashi, *J. Appl. Phys.* **70**, 7119 (1991).
- [9] A. Maldonado, R. Asomoza, J. Canetas-Ortega, E. P. Zironi, R. Hernandez, R. Patino, and O. Solorza-Feria, *Sol. Energy Mater. Sol. Cells* **57**, 331 (1999).
- [10] M. de la L. Olvera, A. Maldonado, R. Asomoza, and M. Melendez-Lira, *Sol. Energy Mater. Sol. Cells* **71**, 61 (2002).
- [11] J. C. Fan and Z. Xie, *Mater. Sci. Eng. B* **150**, 61–665 (2008).

- [12] J. C. Fan and Z. Xie, *Appl. Surf. Sci.* **254**, 6358–6361 (2008).
- [13] Y. Shen, W. Hu, T. Zhang, X. Xu, J. Sun, J. Wu, Z. Ying, and N. Xu, *Mater. Sci. Eng. A* **473**, 201–205 (2008).
- [14] D. C. Look, *Mater. Sci. Eng. B* **80**, 383 (2001).
- [15] V. Vaithianathan and B. T. Lee, *Appl. Phys. Lett.* **88**, 112103 (2006).
- [16] S. Limpijumnong, S. B. Zhang, S. H. Wei, and C. H. Park, *Phys. Rev. Lett.* **92**, 155504 (2004).
- [17] L. Wang, Y. Pu, Y. F. Chen, C. L. Mo, W. Q. Fang, C. B. Xiong, J. N. Dai, and F. Y. Jiang, *J. Cryst. Growth* **284**, 459 (2005).
- [18] N. Gopalakrishnan, B. C. Shin, H. S. Lim, G. Y. Kim, and Y. S. Yu, *Phys. B* **376/377**, 756 (2006).
- [19] B. K. Meyer, H. Alves, D. M. Hofmann, W. Kriegseis, D. Forster, F. Bertram, J. Christen, A. Hoffmann, M. Straburg, M. Dworzak, U. Haboeck, and A. V. Rodina, *Phys. Status Solidi B* **241**, 231 (2004).
- [20] J. C. Sun, J. M. Bian, H. W. Liang, J. Z. Zhao, L. Z. Hu, Z. W. Zhao, W. F. Liu, and G. T. Du, *Appl. Surf. Sci.* **253**, 5161 (2007).
- [21] E. G. Bylander, *J. Appl. Phys.* **49**, 1188 (1978).
- [22] D. C. Look, J. W. Hemsky, and J. R. Sizelove, *Phys. Rev. Lett.* **82**, 2552 (1999).
- [23] D. C. Reynolds, D. C. Look, B. Jogai, and T. C. Collins, *Appl. Phys. Lett.* **79**, 3794 (2001).
- [24] W. Lee, M.-C. Jeong, and J.-M. Myoung, *Appl. Phys. Lett.* **85**, 6167 (2004).
- [25] Y. R. Ryu, T. S. Lee, and H. W. White, *Appl. Phys. Lett.* **83**, 87 (2003).
- [26] D.-K. Hwang, H.-S. Kim, J.-H. Lim, J.-Y. Oh, J.-H. Yang, S.-J. Park, K. K. Kim, D. C. Look, and Y. S. Park, *Appl. Phys. Lett.* **86**, 151917 (2005).
- [27] K. Thonke, T. Gruber, N. Trofilov, R. Schonfelder, A. Waag, and R. Sauer, *Phys. B* **308-310**, 945 (2001).
- [28] W. Y. Liang and A. D. Yoffe, *Phys. Rev. Lett.* **20**, 59 (1968).
- [29] L. Dai, H. Deng, G. Chen, and J. Chen, *Appl. Surf. Sci.* **254**, 1599 (2008).
- [30] H. S. Kang, G. H. Kim, D. L. Kim, H. W. Chang, B. D. Ahn, and S. Y. Lee, *Appl. Phys. Lett.* **89**, 181103 (2006).